PHYSICS

Atomic-scale interface engineering of Majorana edge modes in a 2D magnet-superconductor hybrid system

Alexandra Palacio-Morales[1]*, Eric Mascot[2], Sagen Cocklin[2], Howon Kim[1†], Stephan Rachel[3], Dirk K. Morr[2†], Roland Wiesendanger[1†]

Topological superconductors are predicted to harbor exotic boundary states—Majorana zero-energy modes—whose non-Abelian braiding statistics present a new paradigm for the realization of topological quantum computing. Using low-temperature scanning tunneling spectroscopy, here, we report on the direct real-space visualization of chiral Majorana edge states in a monolayer topological superconductor, a prototypical magnet-superconductor hybrid system composed of nanoscale Fe islands of monoatomic height on a Re(0001)-O(2 × 1) surface. In particular, we demonstrate that interface engineering by an atomically thin oxide layer is crucial for driving the hybrid system into a topologically nontrivial state as confirmed by theoretical calculations of the topological invariant, the Chern number.

INTRODUCTION

Majorana zero-energy modes in topological superconductors are currently attracting great scientific interest because of their potential application in topological quantum information processing based on their non-Abelian quantum exchange statistics (*1*–*7*). Recently, a promising new route to the creation of topological superconductors has been opened in one-dimensional (1D) nanoscale hybrid systems. The reported observation of zero-energy Majorana bound states at the ends of 1D Rashba-nanowire heterostructures (*8*–*10*) and of chains of magnetic adatoms on the surface of s-wave superconductors (*11*–*14*) has provided the proof of concept for the creation of these exotic quasiparticles in condensed matter systems. Similarly, it was proposed that 2D topological superconductors can be created by placing islands of magnetic adatoms on the surface of s-wave superconductors (see Fig. 1A) (*15*–*19*). In these systems, chiral Majorana modes—the variant of Majorana zero-energy states in 2D—are predicted to be localized near the edge of the island (see Fig. 1A) and to form a dispersing 1D mode along the edge that traverses the superconducting gap (Fig. 1B). This, in turn, opens new possibilities for the experimental identification of Majorana modes, as they are expected to exhibit a characteristic energy and spatial structure and to be robust against edge disorder, two properties that can be uniquely explored and visualized via scanning tunneling spectroscopy (STS). Moreover, the ability to use atomic manipulation techniques (*12*, *20*) to create islands of particular shapes, and to control their disorder at the atomic scale, as well as the possibility to spatially move Majorana states through the creation of superconducting vortices (*3*, *5*, *17*), opens unprecedented opportunities for the quantum design of Majorana modes in these heterostructures.

To demonstrate the creation of topological superconductivity and the ensuing chiral Majorana modes through interface engineering in 2D magnet-superconductor hybrid structures, we have grown nanoscale Fe islands of monoatomic height on the (2 × 1) oxygen-reconstructed (0001) surface of the s-wave superconductor Re under ultrahigh vacuum (UHV) conditions. The insertion of an atomically thin oxide separation layer between the magnetic Fe island and the superconducting Re surface is shown to be crucial for the emergence of a topologically nontrivial superconducting state, which is absent when the Fe island is deposited directly on the surface of the superconducting Re substrate. The spatially and energy-resolved differential tunneling conductance, dI/dU, was measured in situ using a low-temperature scanning tunneling microscope (STM) with a superconducting Nb tip to improve the energy resolution (Materials and Methods).

RESULTS AND DISCUSSION

A constant-current STM image of the Fe/Re(0001)-O(2 × 1) hybrid system with a single nanoscale Fe island is shown in Fig. 1C. In general, it is not possible to identify the relative positions of the Fe and O atoms with respect to the Re surface atoms from STM images. However, density functional theory studies (*21*) suggest that the O atoms are located above the hexagonal close-packed (hcp) hollow sites of the Re(0001) surface, forming a p(2 × 1) structure, as confirmed by topographic surface profiles from the STM image (see section S1). Moreover, our theoretical analysis discussed below suggests that the Fe atoms are located directly above the surface Re atoms, thereby continuing the "A-B-A-B" layer stacking of the Re bulk lattice with the intermediate O atoms located above the Re hcp hollow sites. The resulting atomic structure of the hybrid system is displayed in Fig. 1D. The raw dI/dU measured above the O(2 × 1) surface with a superconducting tip is shown in Fig. 1E. To account for the energy dependence of the density of states in the tip, we deconvolute the raw dI/dU using standard methods (see section S3), yielding the deconvoluted dI/dU shown in Fig. 1F. The energies of the coherence peaks reveal a superconducting gap of $\Delta_{O(2\times1)} \approx 280$ μeV, which is slightly lower than that measured on the pure Re(0001) surface ($\Delta_{Re} \approx 330$ μeV). Spectroscopic measurements on different structural domains of the O(2 × 1) layer indicate a uniform spatial distribution of the superconducting gap.

A necessary requirement for the emergence of topological superconductivity is that the Fe islands couple magnetically to the superconducting Re surface. The observation in dI/dU of a Yu-Shiba-Rusinov (YSR) in-gap state (*22*–*26*) near an isolated magnetic Fe adatom located on top of the O(2 × 1) surface demonstrates the existence of the magnetic coupling to the superconducting Re surface, despite the presence of an intermediate oxide layer (see section S1). Moreover, the presence

[1]Department of Physics, University of Hamburg, D-20355 Hamburg, Germany. [2]Department of Physics, University of Illinois at Chicago, 845 W. Taylor St. M/C 273, Chicago, IL, USA. [3]School of Physics, University of Melbourne, Parkville, VIC 3010, Australia.
*Present address: Sorbonne Université, UPMC Université Paris 06, CNRS-UMR 7588, Institut des NanoSciences de Paris, 4 Place Jussieu, 75005 Paris, France.
†Corresponding author. Email: wiesendanger@physnet.uni-hamburg.de (R.W.); hkim@physnet.uni-hamburg.de (H.K.); dkmorr@uic.edu (D.K.M.)

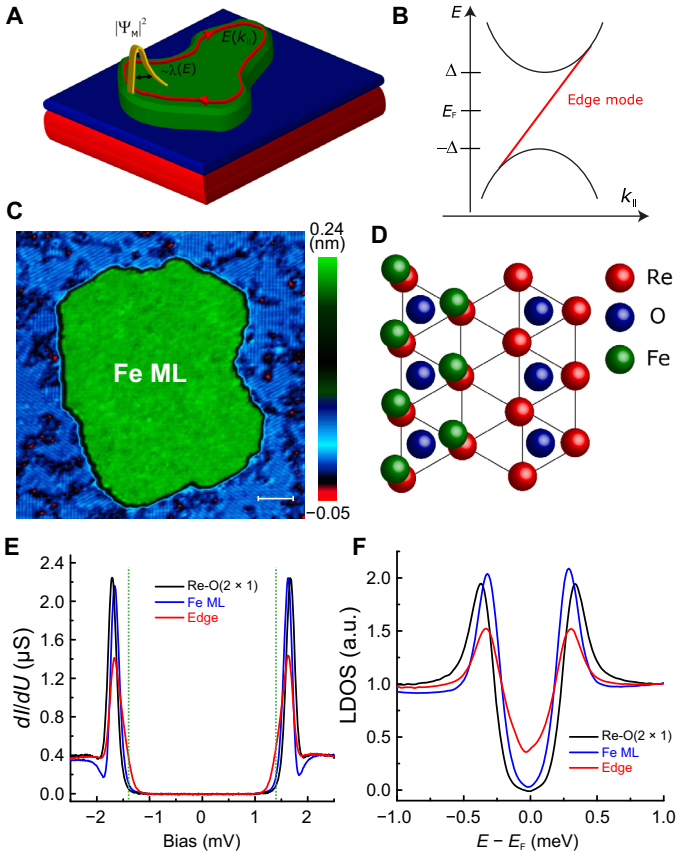

Fig. 1. Chiral Majorana edge modes and the structure of the nanoscale magnet-superconductor hybrid system Fe/Re(0001)-O(2 × 1). (**A**) Schematic picture of the Fe/Re(0001)-O(2 × 1) hybrid system, indicating the spatial structure of the Majorana edge modes and their spatial decay into the center of the island. Here, $k_{\parallel}$ is the mode's momentum parallel to the edge. (**B**) Schematic picture of the edge mode's dispersion, traversing the superconducting bulk gap. (**C**) Constant-current scanning tunneling microscope (STM) image of a small Fe island located on the O (2 × 1)-reconstructed surface of Re(0001). Scale bar, 5 nm. (**D**) Atomic model of the hybrid system, with the Re(0001) substrate (red spheres), p(2 × 1) oxide layer (blue spheres representing O atoms), and Fe adatoms (green spheres). O atoms are located above the Re hexagonal close-packed hollow sites, and Fe adatoms are located above the Re atoms. Lattice constant of the Re(0001) surface: a_{Re} = 0.274 nm. (**E**) Experimentally measured *dI*/*dU* spectrum on the O(2 × 1) surface (black line), in the center (blue line), and at the edge (red line) of the Fe island. As all STS measurements were performed with a superconducting Nb tip whose gap size is Δ_{tip}^{Nb} = 1.41 meV (green dotted lines at $\pm\Delta_{tip}^{Nb}$), the coherence peaks are located at $\Delta_{tip}^{Nb} + \Delta_{O(2\times1)}$ and $\Delta_{tip}^{Nb} + \Delta_{Fe}$, respectively. This yields a measured superconducting gap of $\Delta_{O(2\times1)} \approx 280$ μeV in the O(2 × 1) layer and of $\Delta_{Fe} \approx 240$ μeV in the center of the Fe island. (**F**) Deconvoluted *dI*/*dU* spectrum on the O(2 × 1) surface (black line), in the center (blue line), and at the edge (red line) of the Fe island. Parameters for constant-current STM images and stabilization conditions for STS measurements: U = 2.5 mV, I = 1.0 nA, and T = 360 mK. LDOS, local density of states; a.u., arbitrary units.

of the nanoscale Fe island gives rise to the formation of a band of YSR states near the O(2 × 1) gap edge (*17*). As a result, *dI*/*dU* measured in the middle of the Fe island reveals a smaller superconducting gap $\Delta_{Fe} \approx 240$ μeV than that of the O(2 × 1) layer (see Fig. 1F).

A hallmark of 2D topological superconductors is the existence of dispersive, in-gap Majorana modes that are spatially located along the edges of the system (Fig. 1, A and B) (*15*, *17*, *27*). To visualize the existence of these modes, we present the raw (Fig. 2, A to F) and deconvoluted (Fig. 2, G to L) spatially resolved differential tunneling conductance, in and around the nanoscale Fe island shown in Fig. 1C, with increasing energy, from E_F up to the energy of the coherence peak at Δ_{Fe}. At E_F (Fig. 2G), the *dI*/*dU* map exhibits a large intensity along the edge of the Fe island (confined to within a distance of 5 nm from the edge), indicating the existence of an in-gap edge mode expected for a topological superconductor. With increasing energy (Fig. 2, H and I), the edge mode begins to extend further into the island, consistent with an increase in the mode's localization length, λ(*E*) (Fig. 1A) (see discussion below). Note that the *dI*/*dU* measured inside the Fe island and along the edge is of similar intensity already for energies below Δ_{Fe}, when the localization length becomes comparable to the size of the Fe island (Fig. 2J, $E \approx \pm 140$ μeV; see discussion below). Increasing the energy even further reverses the intensity pattern, such that at the energy of the coherence peaks $\Delta_{Fe} \approx \pm 240$ μeV (Fig. 2L), the *dI*/*dU* intensity at the edge is smaller than that in the island's center. The observation of a topological edge mode in Fe islands on a Re(0001)-O(2 × 1) surface is a universal feature that is not limited to a specific Fe island or particular type of probe tip (see section S2).

To theoretically understand the origin of the combined spatial and energy distribution of the experimentally observed differential tunneling conductance, we consider the Hamiltonian $H = H_{Re} + H_{Fe} + H_{FeRe}$ (for details and parameters, see section S4), where H_{Re} (H_{Fe}) describes the real-space intra- and interorbital hopping elements, the spin-orbit coupling, and superconducting pairing in the Re 5d orbitals (Fe 3d orbitals) and H_{FeRe} represents the electronic hopping/hybridization between the Re surface and the Fe island. As the magnetic structure of the Fe island cannot be deduced from the experimental STS data obtained with a superconducting Nb tip, we consider two magnetic structures for the Fe magnetic moments, which are typically observed on surfaces: a ferromagnetic, out-of-plane alignment structure (*28*) and a 120° Néel-ordered in-plane structure (*29*). To directly compare the theoretically computed local density of states (LDOS) with the experimental results, we consider an Fe island with the same lattice structure and number of atoms as studied experimentally that is located on a Re(0001)-O(2 × 1) surface. We model the influence of the intermediate O(2 × 1) layer through a modification of the hybridization described by H_{FeRe}.

For a ferromagnetic structure, the theoretically computed spatial and energy dependence of the LDOS (Fig. 2, M to R) agrees well with that of the deconvoluted experimental differential tunneling conductance (Fig. 2, G to L). Similarly, the theoretically computed LDOS inside the Fe island and of the bare Re(0001)-O(2 × 1) surface also shows a reduction of the superconducting gap in the former (see section S4), in agreement with the experimental findings (Fig. 1F). Moreover, computing the topological invariant (*30*) (see section S4) for the parameters used in Fig. 2, M to R, we obtain a Chern number $C = 20$. Together, these results strongly suggest that the edge modes shown in Fig. 2 are chiral Majorana modes arising from an underlying topological superconducting state in the Fe/Re(0001)-O(2 × 1) hybrid system. Note that uncertainties in the band parameters and, in particular, in the hybridization strength might affect the actual value of the Chern number but will not result in a topologically trivial phase (see discussion below). Similarly, we find that the system is a topological superconductor for a 120° Néel-ordered in-plane structure (*29*) of the Fe moments (see section S5). Since the energy and spatial dependences of the edge modes similar to those shown in Fig. 2 (M to R) are also found in generic models of topological superconductors (see section S6) (*17*), they should be considered a universal feature of topological superconductivity.

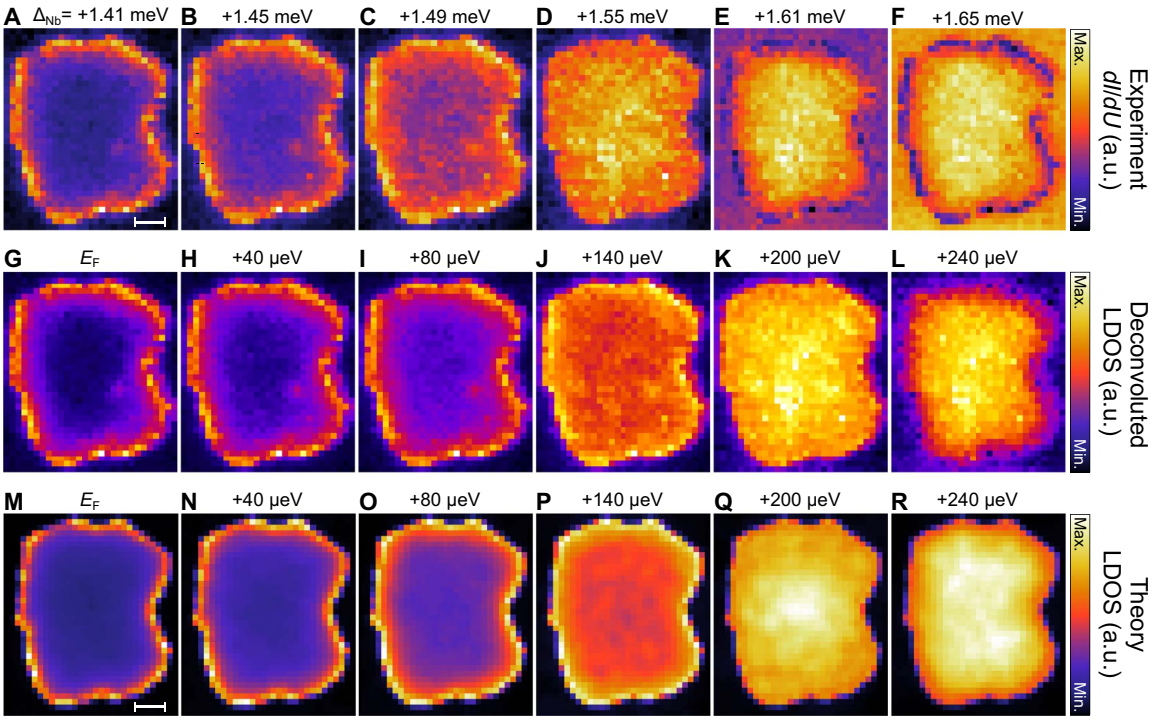

Fig. 2. Evolution of the chiral edge states for the hybrid system Fe/Re(0001)-O(2 × 1) with increasing energy. (**A** to **F**) Experimentally measured differential tunneling conductance maps and (**G** to **L**) corresponding deconvoluted datasets (see section S3) for the Fe island shown in Fig. 1C from the Fermi level, $E_F = \Delta_{tip}^{Nb}$ to Δ_{Fe} = 240 μeV above E_F. At low energies (A to C and G to I), the *dI*/*dU* map reveals states that are localized along the edges of the Fe island (edge modes). Once the localization length of the edge modes becomes of the size of the island (D and J), the *dI*/*dU* in the center of the island is comparable to that along the edges. (**M** to **R**) Theoretically computed spatially resolved LDOS for the same energies as in (G) to (L). The theoretical data have been spatially convoluted to reproduce the experimental spatial resolution (see section S4). STS measurement conditions: U = 2.5 mV, I = 1.0 nA, and T = 360 mK. The intensity scale is adjusted for each figure separately. Scale bars, 5 nm (A and M).

A further important signature of Majorana modes is that they are topologically protected against edge disorder according to the bulk-boundary correspondence (*27*). Edge modes that have a trivial, nontopological origin can easily be moved away from the Fermi energy or even be destroyed by disorder. However, the experimentally studied Fe island does not only have a spatial symmetry different from the underlying Re(0001)-O(2 × 1) surface but also exhibits a large degree of disorder along its edges (Fig. 1C). The fact that edge modes are observed at E_F despite this disorder further supports our conclusion that these modes are topologically protected chiral Majorana modes.

To further elucidate the properties of the Majorana edge modes, we present in Fig. 3 the deconvoluted differential tunneling conductance (Fig. 3A) and the theoretically calculated LDOS (Fig. 3B) for increasing energy along a cut through the Fe island, as shown in the insets [the surface profile of the island is shown in the bottom panels of Fig. 3 (A and B)]. Both quantities agree quantitatively and decay as expected exponentially into the island with a localization length $\lambda(E)$ (as sketched in Fig. 1A) that increases with increasing energy. The maxima in *dI*/*dU* and the LDOS are located right at the edge of the island for all energies, as expected from generic models of topological superconductors with a dominant s-wave order parameter (see section S6) (*18*). This very good agreement between the topographically determined edge of the Fe island and the maximum in *dI*/*dU* therefore provides additional evidence for the topological nature of the edge modes. Note that the recently reported spatial splitting of the edge mode (*18*) can only be understood if one assumes a topological superconductor with a predominant p-wave order parameter (*18*) or if the edge mode starts to hybridize with bulk states (*19*).

The question naturally arises to what extent the observed topological superconducting phase of the Fe/Re(0001)-O(2 × 1) hybrid system is robust against variations in the strength of parameters, such as the hybridization between the Re surface and the Fe island, V_{FeRe}, which is mediated by the O(2 × 1) oxide layer, or the chemical potentials, μ_{Fe} or μ_{Re}. To investigate this question, we present in Fig. 3C the topological phase diagram of the system, as a function of V_{FeRe} and μ_{Fe} (the Chern number was calculated as described in section S4, and the parameters for the system considered above are indicated by a yellow circle). The phase diagram reveals an abundance of topological superconducting phases in close proximity to each other that are characterized by different Chern numbers. While the uncertainty in the electronic band parameters we have used to describe the Fe/Re(0001)-O(2 × 1) system can result in an uncertainty of the actual Chern number in the experimentally realized system, the fact that the system resides in a topological phase is robust. This substantiates our conclusion that the observed edge modes directly reflect the topological nature of the magnet-superconductor hybrid system.

To demonstrate that interface engineering using an atomically thin oxide layer is crucial for the emergence of topological superconductivity in the Fe/Re(0001)-O(2 × 1) hybrid system, we contrast the above results with those obtained when the Fe layer is directly deposited on the Re(0001) surface without an intermediate oxide layer (see Fig. 4) (*29*). In this case, with the Fe atoms being located directly above the Re(0001) hcp hollow sites (Fig. 4H), *dI*/*dU* measured on the Fe islands exhibits no signature of edge modes in the raw data (Fig. 4, E to G) and in the deconvoluted data (Fig. 4, I to K); rather it reflects delocalized, bulk-like excitations throughout the entire Fe island at E_F.

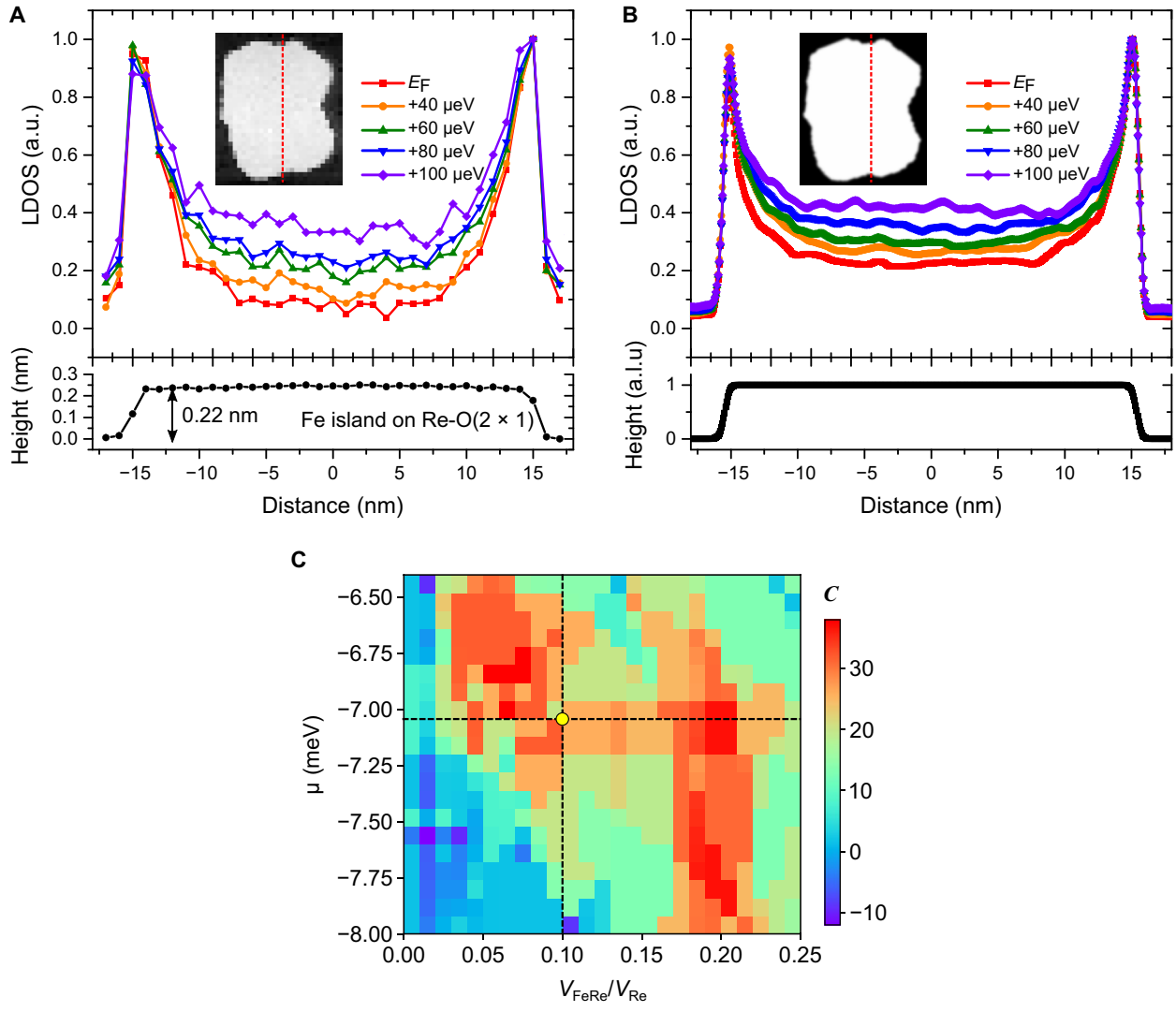

Fig. 3. Decay of the chiral edge states inside an Fe island. (**A**) Deconvoluted LDOS profiles obtained from the experimentally measured *dI*/*dU* spectra along the red dotted line in the inset for several different energies: E_F, +40 μeV, +60 μeV, +80 μeV, and +100 μeV. (**B**) Theoretically computed LDOS along the red line in the inset for the same energies as in (A). The corresponding surface profiles of the island are depicted in the bottom panels of (A) and (B). The theoretical results have been spatially convoluted to reproduce the experimental spatial resolution (see section S4). Insets in (A) and (B): The STM topography image and theoretically considered model structure of an Fe island, respectively. All LDOS profiles in (A) and (B) are normalized by their maximum values at the island's edge. (**C**) Theoretical phase diagram of the hybrid system. Chern number for an out-of-plane ferromagnetic structure of the Fe layer, as a function of V_{FeRe}/V_{Re} and μ_{Fe} (see section S4). The phase diagram reveals an abundance of topological phases near the parameter set used to describe the Fe/Re(0001)-O(2 × 1) hybrid system (yellow dot with crossed dotted lines).

Our theoretical analysis of this system reveals (using the same set of parameters as for Fig. 2, M to R) that the change in the spatial location of the Fe atoms with respect to the Re(0001) surface (arising from the missing intermediate oxide layer) renders the electronic structure of this hybrid system gapless. As a result, the LDOS at E_F is nonzero, leading to the delocalized excitations observed experimentally. Moreover, the absence of a gap implies that the system is in a trivial, nontopological phase, explaining the absence of edge modes, as observed experimentally. Thus, the change in the relative position of the Fe and Re atoms induced by the presence of the oxide layer is crucial for realizing topological superconductivity in the hybrid system.

In conclusion, we reported the engineering of topological superconductivity and direct visualization of theoretically predicted Majorana edge modes in a nanoscale Fe island located on a Re(0001)-O(2 × 1) substrate. The combination of spatially resolved spectroscopy and topographic information allowed us to not only correlate for the first time the energy and spatial dependence of the observed in-gap edge modes with the physical edge of the Fe island but also demonstrate the robustness of these edge modes against edge disorder [no topographic information was available in a previous study using Pb/Co/Si(111) heterostructures (*18*)]. Both of these experimental observations, which are in very good agreement with our theoretical calculations, represent hallmarks of the modes' topological nature. Our theoretical studies also demonstrate that the emergence of topological superconductivity in Fe/Re(0001)-O(2 × 1) does not require any fine-tuning of parameters but is expected over a wide range of band parameters and magnetic structures. Moreover, we demonstrated that the emergence of topological superconductivity in such a hybrid magnet-superconductor system is only made possible

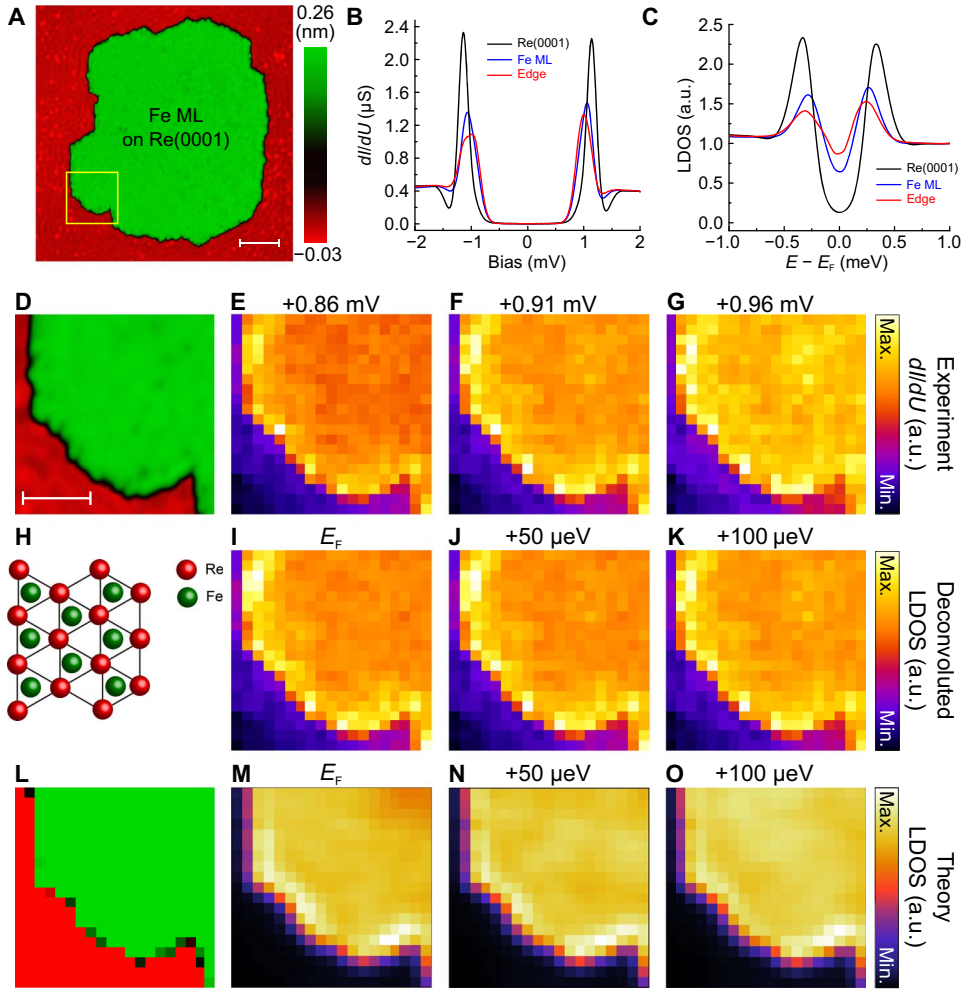

Fig. 4. Topological trivial Fe island on a bare Re(0001) surface. (**A**) The STM image of the Fe island being in direct contact with the superconducting Re substrate. Scale bar, 10 nm. (**B**) Experimentally measured *dI*/*dU* spectra on the clean Re(0001) surface (black), at the center (blue), and at the edge (red) of the Fe island using a superconducting Nb tip whose gap size is $\Delta_{tip}^{Nb} = 0.86$meV (see section S3). Tunneling conditions for STM/STS measurements: $U = 2.0$ mV, $I = 1.0$ nA, and $T = 360$ mK. (**C**) The deconvoluted surface LDOS derived from the spectra shown in (B) taking into account the superconducting gap of the Nb tip used for the STS measurements (see section S3). (**D**) A zoomed-in STM image of the Fe island shown in (A) [yellow boxed area in (A)]. Scale bar, 5 nm. (**E** to **G**) Experimentally measured *dI*/*dU* maps for the Fe island shown in (D) at $U = +0.86$, +0.91, and +0.96 mV, which are corresponding to the energy of E_F, 50 μeV, and 100 μeV, respectively. (**H**) Atomic model of the Fe island on the bare Re(0001) substrate. Fe adatoms are located at the hollow sites of the Re substrate. (**I** to **K**) The spatial distribution of the deconvoluted surface LDOS for the island shown in (D). (**L**) The zoomed-in image of the theoretically considered Fe island structure, reproducing the experimental Fe island in (D). (**M** to **O**) Calculated LDOS of the island shown in (L) at the same energies as the experimental results. The theoretical data have been spatially convoluted to reproduce the experimental spatial resolution (see section S4).

through interface engineering using an atomically thin separation layer. The direct real-space visualization of chiral Majorana edge modes demonstrated here, in combination with STM-based single-atom manipulation techniques (*12*, *20*), opens unprecedented opportunities to realize topological phases in artificial 2D magnetic adatom arrays on elemental superconducting substrates providing fascinating building blocks for future topological quantum computer architectures.

MATERIALS AND METHODS

Preparation of the model-type hybrid sample and the STM tip

An atomically clean Re(0001) surface was prepared in UHV by repeated cycles of Ar^+ ion sputtering and annealing at temperatures between 1150°C and 1250°C followed by flashing the substrate at 1530°C (*31*). The surface cleanliness was checked in situ by STM after transferring the sample into the cryostat. The ultrathin oxide layer was grown by flashing the Re single crystal in an O_2 atmosphere (pressure range, $10^{-9} \sim 10^{-10}$ mbar) (*32*). Fe was deposited by electron beam evaporation from a pure Fe rod (>99.99%) yielding a coverage of about 0.4 monolayers.

The Nb tip used for the STM/STS experiments was mechanically cut ex situ at ambient conditions and then inserted into the UHV system. It was conditioned by applying voltage pulses (a few Volts for 50 ms) and gentle indentation into the Re(0001) surface. Its quality was judged acceptable if a sufficiently large Nb gap could be reproduced and no in-gap states were observed in the tunneling spectra obtained on the Re(0001) surface.

STM/STS data acquisition

The experiments were carried out in a ^{3}He-cooled low-temperature STM system (USM-1300S, Unisoku, Japan) operating at $T = 360$ mK

under UHV conditions. Spectroscopic data were obtained by measuring the differential tunneling conductance (dI/dU) using a standard lock-in technique with a bias modulation voltage of 20 μV_{rms} and a frequency of 841 Hz with opened feedback loop. The bias voltage was applied to the sample, and the tunneling current was measured through the tip using a commercially available controller (Nanonis, SPECS, Swiss).

SUPPLEMENTARY MATERIALS

Supplementary material for this article is available at http://advances.sciencemag.org/cgi/content/full/5/7/eaav6600/DC1

Section S1. Surface characterization of Fe/Re(0001)-O(2 × 1)
Section S2. Universal topological nature of Fe islands/Re-O hybrid system
Section S3. Deconvolution procedure of the tunneling spectra for the superconductor-superconductor tunnel junctions
Section S4. Theoretical model
Section S5. Magnetic structure of the Fe island and topological superconductivity
Section S6. Evolution of topological Majorana modes in a generic topological superconductor
Fig. S1. STM/STS characterization of the Re(0001)-O(2 × 1) surface.
Fig. S2. Another example of a topological nontrivial Fe island on a Re(0001)-O(2 × 1) surface.
Fig. S3. Deconvoluted tunneling spectra and LDOS maps depending on the parameter γ.
Fig. S4. Theoretically computed LDOS.
Fig. S5. Topological phase diagram.
Fig. S6. Spatially resolved LDOS at E_F of a magnetically disordered Fe island.
Fig. S7. Energy evolution of the spatially resolved LDOS for a generic topological superconductor.
Table S1. Tight binding parameters for the Fe/Re(0001)-O(2 × 1) hybrid system.
References (*33*–*41*)

REFERENCES AND NOTES

1. C. Nayak, S. H. Simon, A. Stern, M. Freedman, S. Das Sarma, Non-Abelian anyons and topological quantum computation. *Rev. Mod. Phys.* **80**, 1083–1159 (2008).
2. C. W. J. Beenakker, Search for Majorana fermions in superconductors. *Annu. Rev. Condens. Matter Phys.* **4**, 113–136 (2013).
3. J. Alicea, New directions in the pursuit of Majorana fermions in solid state systems. *Rep. Prog. Phys.* **75**, 076501 (2012).
4. F. Wilczek, Majorana returns. *Nat. Phys.* **5**, 614–618 (2009).
5. D. A. Ivanov, Non-abelian statistics of half-quantum vortices in *p*-wave superconductors. *Phys. Rev. Lett.* **86**, 268–271 (2001).
6. S. R. Elliott, M. Franz, *Colloquium*: Majorana fermions in nuclear, particle, and solid-state physics. *Rev. Mod. Phys.* **87**, 137–163 (2015).
7. M. Sato, Y. Ando, Topological superconductors: A review. *Rep. Prog. Phys.* **80**, 076501 (2017).
8. R. M. Lutchyn, J. D. Sau, S. Das Sarma, Majorana fermions and a topological phase transition in semiconductor-superconductor heterostructures. *Phys. Rev. Lett.* **105**, 077001 (2010).
9. Y. Oreg, G. Refael, F. von Oppen, Helical liquids and Majorana bound states in quantum wires. *Phys. Rev. Lett.* **105**, 177002 (2010).
10. V. Mourik, K. Zuo, S. M. Frolov, S. R. Plissard, E. P. A. M. Bakkers, L. P. Kouwenhoven, Signatures of Majorana fermions in hybrid superconductor-semiconductor nanowire devices. *Science* **336**, 1003–1007 (2012).
11. S. Nadj-Perge, I. K. Drozdov, J. Li, H. Chen, S. Jeon, J. Seo, A. H. MacDonald, B. A. Bernevig, A. Yazdani, Observation of Majorana fermions in ferromagnetic atomic chains on a superconductor. *Science* **346**, 602–607 (2014).
12. H. Kim, A. Palacio-Morales, T. Posske, L. Rózsa, K. Palotás, L. Szunyogh, M. Thorwart, R. Wiesendanger, Toward tailoring Majorana bound states in artificially constructed magnetic atom chains on elemental superconductors. *Sci. Adv.* **4**, eaar5251 (2018).
13. M. Ruby, F. Pientka, Y. Peng, F. von Oppen, B. W. Heinrich, K. J. Franke, End states and subgap structure in proximity-coupled chains of magnetic adatoms. *Phys. Rev. Lett.* **115**, 197204 (2015).
14. R. Pawlak, M. Kisiel, J. Klinovaja, T. Meier, S. Kawai, T. Glatzel, D. Loss, E. Meyer, Probing atomic structure and Majorana wavefunctions in mono-atomic Fe chains on superconducting Pb surface. *npj Quantum Inf.* **2**, 16035 (2016).
15. J. Li, T. Neupert, Z. Wang, A. H. MacDonald, A. Yazdani, B. A. Bernevig, Two-dimensional chiral topological superconductivity in Shiba lattices. *Nat. Commun.* **7**, 12297 (2016).
16. J. Röntynen, T. Ojanen, Topological superconductivity and high chern numbers in 2D ferromagnetic shiba lattices. *Phys. Rev. Lett.* **114**, 236803 (2015).
17. S. Rachel, E. Mascot, S. Cocklin, M. Vojta, D. K. Morr, Quantized charge transport in chiral Majorana edge modes. *Phys. Rev. B.* **96**, 205131 (2017).
18. G. C. Ménard, S. Guissart, C. Brun, R. T. Leriche, M. Trif, F. Debontridder, D. Demaille, D. Roditchev, P. Simon, T. Cren, Two-dimensional topological superconductivity in Pb/Co/Si(111). *Nat. Commun.* **8**, 2040 (2017).
19. K. Björnson, A. M. Black-Schaffer, Probing chiral edge states in topological superconductors through spin-polarized local density of state measurements. *Phys. Rev. B.* **97**, 140504 (2018).
20. D. M. Eigler, E. K. Schweizer, Positioning single atoms with a scanning tunnelling microscope. *Nature* **344**, 524–526 (1990).
21. P. Kaghazchi, T. Jacob, Structure of rhenium surfaces in an oxygen environment. *Phys. Rev. B.* **83**, 035417 (2011).
22. L. Yu, Bound state in superconductors with paramagnetic impurities. *Acta Phys. Sin.* **21**, 75–91 (1965).
23. H. Shiba, Classical spins in superconductors. *Prog. Theor. Phys.* **40**, 435–451 (1968).
24. A. I. Rusinov, On the theory of gapless superconductivity in alloys containing paramagnetic impurities. *Sov. J. Exp. Theor. Phys.* **29**, 1101–1106 (1969).
25. A. V. Balatsky, I. Vekhter, J.-X. Zhu, Impurity-induced states in conventional and unconventional superconductors. *Rev. Mod. Phys.* **78**, 373–433 (2006).
26. L. Cornils, A. Kamlapure, L. Zhou, S. Pradhan, A. A. Khajetoorians, J. Fransson, J. Wiebe, R. Wiesendanger, Spin-resolved spectroscopy of the Yu-Shiba-Rusinov states of individual atoms. *Phys. Rev. Lett.* **119**, 197002 (2017).
27. X.-L. Qi, S.-C. Zhang, Topological insulators and superconductors. *Rev. Mod. Phys.* **83**, 1057–1110 (2011).
28. M. Bode, A. Kubetzka, K. von Bergmann, O. Pietzsch, R. Wiesendanger, Imaging the switching behavior of superparamagnetic nanoislands by spin-polarized scanning tunneling microscopy. *Microsc. Res. Tech.* **66**, 117–125 (2005).
29. A. Palacio-Morales, A. Kubetzka, K. von Bergmann, R. Wiesendanger, Coupling of coexisting noncollinear spin states in the Fe monolayer on Re(0001). *Nano Lett.* **16**, 6252–6256 (2016).
30. G. E. Volovik, An analog of the quantum Hall effect in a superfluid ^{3}He film. *Sov. Phys. JETP.* **67**, 1804–1811 (1988).
31. S. Ouazi, T. Pohlmann, A. Kubetzka, K. von Bergmann, R. Wiesendanger, Scanning tunneling microscopy study of Fe, Co and Cr growth on Re(0001). *Surf. Sci.* **630**, 280–285 (2014).
32. R. Pantel, M. Bujor, J. Bardolle, Oxygen adsorption on various vicinal faces close to the (0001) basal plane of rhenium. *Surf. Sci.* **83**, 228–242 (1979).
33. R. C. Dynes, V. Narayanamurti, J. P. Garno, Direct measurement of quasiparticle-lifetime broadening in a strong-coupled superconductor. *Phys. Rev. Lett.* **41**, 1509–1512 (1978).
34. D.-J. Choi, C. Rubio-Verdú, J. de Bruijckere, M. M. Ugeda, N. Lorente, J. I. Pascual, Mapping the orbital structure of impurity bound states in a superconductor. *Nat. Commun.* **8**, 15175 (2017).
35. D. L. Phillips, A technique for the numerical solution of certain integral equations of the first kind. *J. Assoc. Comput. Mach.* **9**, 84–97 (1962).
36. S. Twomey, On the numerical solution of Fredholm integral equations of the first kind by the inversion of the linear system produced by quadrature. *J. Assoc. Comput. Mach.* **10**, 97–101 (1963).
37. M. Ternes, W.-D. Schneider, J.-C. Cuevas, C. P. Lutz, C. F. Hirjibehedin, A. J. Heinrich, Subgap structure in asymmetric superconducting tunnel junctions. *Phys. Rev. B.* **74**, 132501 (2006).
38. J. C. Slater, G. F. Koster, Simplified LCAO method for the periodic potential problem. *Phys. Rev.* **94**, 1498–1524 (1954).
39. D. A. Papaconstantopoulos, *Handbook of the Band Structure of Elemental Solids: From Z = 1 to Z = 112* (Springer US, Boston, MA, 2015).
40. E. Prodan, Disordered topological insulators: A non-commutative geometry perspective. *J. Phys. A Math. Theor.* **44**, 239601 (2011).
41. T. Hahn, Cuba—A library for multidimensional numerical integration. *Comput. Phys. Commun.* **168**, 78–95 (2005).

Acknowledgments: We would like to thank H. Jeschke and M. Vojta for stimulating discussions. **Funding:** This work was supported by the European Research Council Advanced Grant ASTONISH (project no. 338802) and ADMIRE (project no. 786020); the Alexander von Humboldt foundation; the U.S. Department of Energy, Office of Science, Basic Energy Sciences, under award no. DE-FG02-05ER46225; and the Australian Research Council (FT180100211). This research used resources of the National Energy Research Scientific Computing Center (NERSC), a U.S. Department of Energy Office of Science User Facility operated under contract no. DE-AC02-05CH11231 (to E.M., S.C., and D.K.M.).

Author contributions: A.P.-M. and R.W. conceived and designed the experiments. A.P.-M. and H.K. carried out the STM/STS experiments and processed and analyzed the data. E.M., S.C., S.R., and D.K.M. performed the theoretical modeling. R.W. and D.K.M. supervised the project. All authors discussed the results and contributed to the manuscript. **Competing interests:** The authors declare that they have no competing interests. **Data and materials availability:** All data needed to evaluate the conclusions in the paper are present in the paper and/or the Supplementary Materials. Additional data related to this paper may be requested from the authors.

Submitted 8 October 2018
Accepted 19 June 2019
Published 26 July 2019
10.1126/sciadv.aav6600

Citation: A. Palacio-Morales, E. Mascot, S. Cocklin, H. Kim, S. Rachel, D. K. Morr, R. Wiesendanger, Atomic-scale interface engineering of Majorana edge modes in a 2D magnet-superconductor hybrid system. *Sci. Adv.* **5**, eaav6600 (2019).

Author/s:
Palacio-Morales, A; Mascot, E; Cocklin, S; Kim, H; Rachel, S; Morr, DK; Wiesendanger, R

Title:
Atomic-scale interface engineering of Majorana edge modes in a 2D magnet-superconductor hybrid system

Date:
2019-07-01

Citation:
Palacio-Morales, A., Mascot, E., Cocklin, S., Kim, H., Rachel, S., Morr, D. K. & Wiesendanger, R. (2019). Atomic-scale interface engineering of Majorana edge modes in a 2D magnet-superconductor hybrid system. SCIENCE ADVANCES, 5 (7), https://doi.org/10.1126/sciadv.aav6600.

Persistent Link:
http://hdl.handle.net/11343/249613

File Description:
published version